



Reversibility of Electrowetting on Hydrophobic Surfaces and Dielectrics Under Continuous Applied DC Voltage

Oh-Sun Kwon^{1,2}, Minkyu Kim³, Taeyun Kim³, Chanho Lee³, Sungjin Han³,
Jae-yong Kim², Chan-Hee Jung⁴, Jae-Hak Choi⁴, and Kwanwoo Shin^{1,*}

¹Department of Chemistry, Institute of Biological Interfaces, Sogang University, Seoul 121-742, Korea

²Department of Physics, Hanyang University, Seoul 133-791, Korea

³Korea Science Academy of KAIST, Busan 614-822, Korea

⁴Advanced Radiation Technology Institute, KAERI, Jeongeup 580-185, Korea

Various properties of electrowetting such as reversibility, reproducibility and mobility have been investigated experimentally. A conductive water drop on a thin hydrophobic film of amorphous fluropolymers coated on the counter electrode showed unexpectedly the poor reversibility under the discontinuous voltage, so called the contact angle hysteresis. The hysteresis could not be completely suppressed by inserting additionally a thick parylene-C film which has the high dielectric constant and no pinholes. However, both the reversibility and the reproducibility have been enhanced under the continuous voltage starting from the highest absolute electric potential.

Keywords: Electrowetting, Liquid Drop, Contact Angle Hysteresis, Dielectrics, EWOD.

1. INTRODUCTION

Electrowetting is the spreading of a conductive liquid drop on surface of matter under the external electrostatic field.¹⁻⁴ Though Lippmann discovered this phenomenon in 1875, it has been only a decade to be attracted and developed for liquid lenses, liquid displays, and microfluidic chips.^{1,4,5}

Electrowetting on dielectrics (EWOD) is practically important due to its excellent durability, reproducibility and reversibility.¹⁻⁴ When the voltage is applied to a conductive liquid drop on a rigid dielectric substrate, the contact angle (CA) of the drop is reduced (Fig. 1). According to the classical Young-Lippmann's theory, the CA, θ is given by a quadratic function of voltage, V :

$$\cos \theta(V) = \cos \theta_0 + \frac{1}{2\gamma_{la}} CV^2 \quad (1)$$

where θ_0 is the CA under no electric potential, γ_{la} is the interfacial tension between liquid and environment air phase and C is the capacitance of unit surface area of dielectric underneath the drop. Unfortunately, however, CA cannot be reduced up to zero, i.e., the complete wetting by

increasing V so that there always exists the saturated CA, which has not been completely understood theoretically so far.^{3,4} Experimentally, to improve the EWOD techniques the many materials, such as conductive liquids,^{6,7} electrodes,^{5,8} environmental phases,⁹ and dielectrics,^{2,10-11} have been studied. Very recently ionic liquids have been tested to substitutes for aqueous conductive liquids with its various advantages such as their low volatility, low viscosity and high conductivity.¹² Dielectric materials which were most affective on decreasing driving voltage were also developed.

Here we present the enhancement of reversibility, the reproducibility and mobility of EWOD under the continuous applied DC voltage.

2. EXPERIMENTAL DETAILS

Our experimental setup is shown in Figure 1. We used a glass substrate coated with indium tin oxide (ITO, surface resistivity 20 Ω /sq) as a planar grounded electrode.¹³ The dielectric parylene-C (2 μ m, $\epsilon = 3.0$) was coated on the substrate in chemical vapor polymerization of di-p-xylyene.

For providing a hydrophobic surface, amorphous fluoropolymer polytetrafluoroethylene (PTFE AF 1600,

* Author to whom correspondence should be addressed.

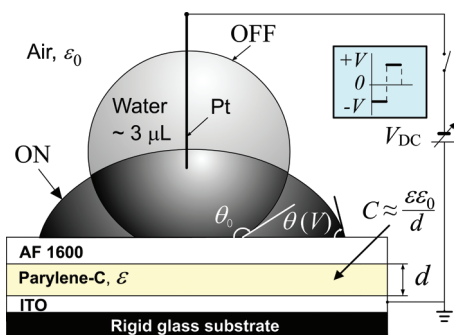


Fig. 1. Experimental setup for CA measurements: Dark and gray colors of the drop correspond to the on and off of the switch, respectively. Inset shows two possible polarities (+V or -V) of DC voltage.

$\epsilon = 1.93$) which was dissolved in perfluoro-2-butyl tetrahydrofuran FC-40 (3M) solvent as 1.0 wt% was subsequently deposited by spin-coating at 2000 rpm for 120 s. The sample immediately was heated in an oven at 90 °C for 15 min to evaporate the solvent and then it was baked in vacuum chamber at 170 °C for 30 min which is slightly

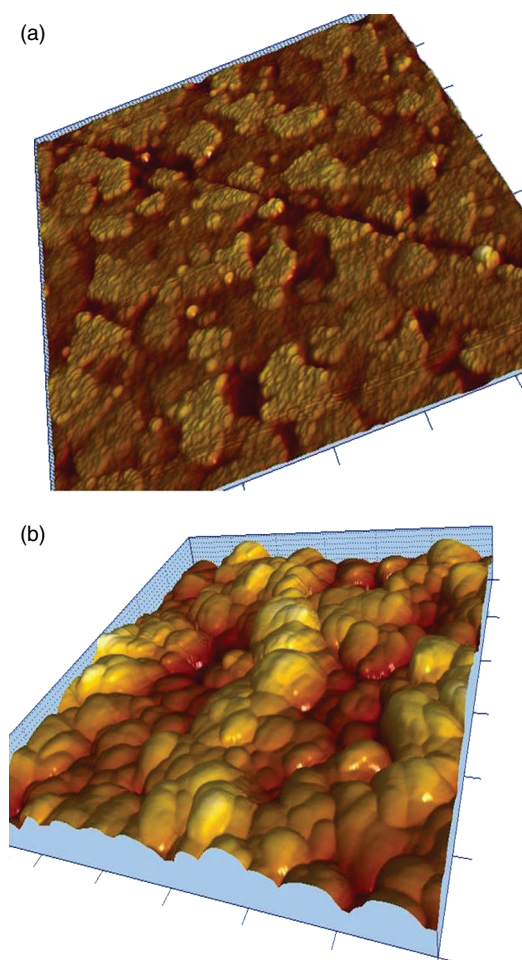


Fig. 2. Comparison of AFM images of surfaces of (a) rough AF 1600 and (b) pinholeless parylene-C. Note that unit of x-, y- and z-tics is 0.5 $\mu\text{m}/\text{div}$.

over the glass transition temperature 160 °C of AF 1600. Thicknesses of AF 1600 films were very thin a typically 200 nm which was measured by using ellipsometry.¹⁴ For comparison typical AFM scanning images of the surfaces of parylene-C and AF 1600 are shown in Figure 2. Pinholeless surface of parylene-C is apparent which is good for protecting leakage of any liquids and increasing electric breakdown voltage due to strengthen dielectric constant, whereas that of AF 1600 has irregularity with rms roughness of 10 nm which is mainly due to dilute weight percent. Platinum (Pt, diameter 50 μm) needle was used for an electrode immersed in a liquid drop. The counter ITO electrode insulated with parylene-C film was well grounded with our whole system. For liquid drops only deionized water (DIW, $\gamma_{\text{la}} = 72 \text{ mN/m}$ and $\rho = 17.2 \text{ M}\Omega \cdot \text{cm}$ at $T = 25^\circ$) has been investigated. Drop size was about 3 μL . For this size of a drop, the gravity effect is ignorable since the Bond number which represents the relative effect of the gravity to the surface tension is less than 10^{-3} . All measurements were conducted at room temperature.

3. RESULTS AND DISCUSSION

The CA data on a thin hydrophobic AF 1600 film are presented in Figure 3(a). The parabolic CA variation at the low voltage of less than 50 V represents well the dependence on applied voltage.

The achieved controllable range of CA is from 115 to 80° under the applied voltage of DC 0–50 V. Such a degree of angular difference of 35° is enough for most applications of electrowetting techniques such as microfluidics, liquid lenses or e-papers.^{1–4} In Figure 3(b), the cosine of CA versus the square of applied voltage is plotted in order to confirm clearly the theoretical prediction. The linearity obtained from the curve fitting only with CA data under 50 V represents that the measured CA data are in good

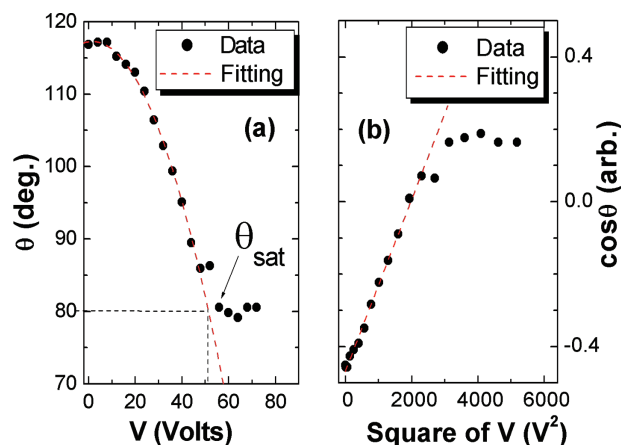


Fig. 3. For a thin film of PTFE AF 1600, (a) CA data with a parabolic curve fitting and (b) $\cos \theta$ data with a linear curve fitting.

agreement with the Young-Lippmann's equation in Eq. (1) as well Figure 1(a).

As the voltage slightly greater than 50 V, the CA always reached to the limited value 80° , so called the CA saturation, θ_{sat} . Though numerous hypotheses for saturation of CA, such as, the ion trap,² the zero interfacial tension^{6, 15} have been proposed, it however has been not still clearly understood so far. Our result is good agreement to the Quinn's model of vanishing interfacial tension between liquid and substrate at saturation.

When the applied voltage reached to 100 V a few of evaporating water vapors appeared inside of the drop, indicating the dielectric breakdowns of insulation of $0.2 \mu\text{m}$ AF 1600 film since the dielectric breakdown strength of AF 1600 is $20 \text{ V}/\mu\text{m}$. They are different from the electric short failures caused by the pinholes on AF 1600 surface as shown in the AFM image in Figure 2(a).

To investigate the reproducibility of CA, three initial cyclic CA measurements with a cycle composed of advancing and receding CA corresponding to increasing and decreasing voltage respectively were performed on a flesh surface and the results are presented in Figure 4.

At first we note the highest initial CA, 120° , at 0 V which was observed only once at the very flesh surface. When the first cycle measurement was completed, this maximum CA value under no voltage was disappeared completely and reduced to about 115° but with the high deviation. This instability at low voltage seems to be caused by the surface friction at the contact line. Except the instability at low voltage, 0–10 V, the CA data are very reversible and reproducible under the cyclic applied voltage since they show high symmetry about 0 V with the identical parabolic shape.

To enhance the dielectric strength and water resistive a relative $2 \mu\text{m}$ thick dielectric parylene-C film was inserted between AF 1600 and ITO electrode. Parylene-C has been used widely in electronics as a good insulating film due to its high electric breakdown strength, $270 \text{ V}/\mu\text{m}$.^{2, 3} The

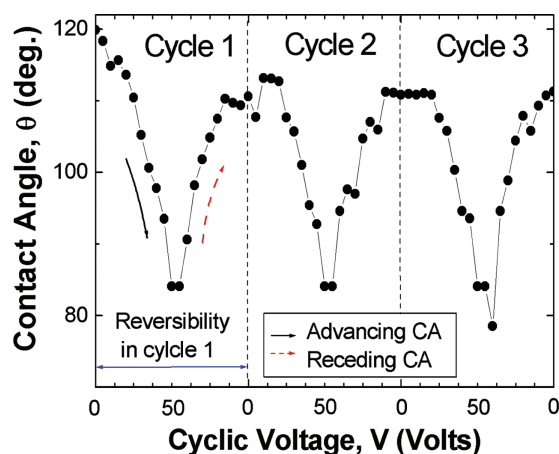


Fig. 4. Reversibility and reproducibility of CA data in the initial 3 cyclic CA measurements.

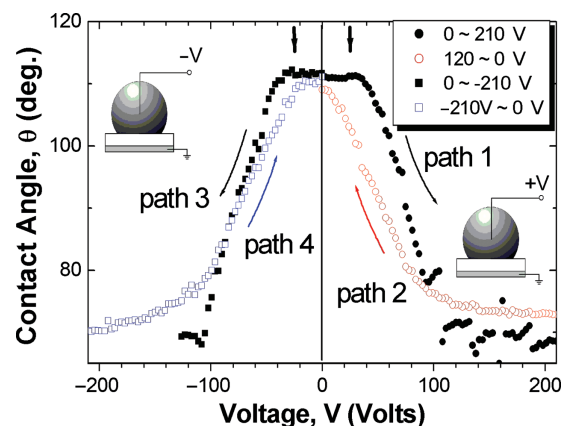


Fig. 5. The CA variations in four distinct paths along applied voltage. Path 1 and 2 and path 3 and 4 are under the positive and negative electric potential on water drops respectively with respect to the grounded counter electrode.

CA data for DIW drops on this multilayer are presented in Figure 5. In order to investigate the symmetry, reversibility and mobility of the water drops in EWOD in detail, the CA measurements were separated into four distinct paths with the combination of both the polarity ($\pm V$) and the increment ($\pm \Delta V$) for the voltage applied on the Pt-electrode. For convenience, they were denoted as the path 1 and 3 for advancing CA's and path 2 and 4 for receding CA's. The advancing CA means that the CA data are measured as the voltage is applied from the zero potential to $+V$ or $-V$ and the receding CA is vice versa. In electrostatic view point, they correspond to the processes of charging and discharging the free ions on the liquid electrode of the planar dielectric capacitor respectively (see Fig. 1). Note that to obtain the n^{th} CA value, $\theta_n(V_n)$, we applied the voltage with continuous increments, such as from V_{n-1} to V_n in $V_n = V_0 + (n-1)\Delta V$ with $V_0 = 0$, not to jump from the grounded reference potential directly to V_n all the time during a set of measurement. We found that some noticeable features in EWOD data under this continuous voltage scheme, which were related to these four different paths, as follows.

Evaporation of a water drop completely disappeared due to high dielectric breakdown strength and pinhole free surface of parylene-C (Fig. 2(b)). At the low voltage of less than ± 25 V, the CA variations appeared apparently in the smooth parabolic curves in the receding path 2 and 4, whereas the change of CA was unstable in the advancing path 1 and 3.

As expected, however, each pair of advancing path 1 and 3 and receding path 2 and 4 is highly symmetric about 0 V with the maximum 110° and 113° in CA separately. At high voltage near to ± 100 V, the CA reaches to a saturated value about $70\text{--}80^\circ$, regardless of paths. The high symmetry about y-axis indicates that switching polarities of Pt-electrode has the indistinguishable effects on the capacitance of the dielectric film. Consequently, it means that

there would be no distinguishable if the alternating current (AC) voltage is applied instead of DC voltage on a conducting water drop, which is, in fact, implied in the quadratic feature of Eq. (1).

The high reversibility between advancing and receding CA in DC voltage on AF 1600 films has been reported in many literatures.² In our experiments, however, the reversibility couldn't be achieved satisfactory in the path 1–2 for positive electric potential as well as the path 3–4 for negative potential, though the latter is relatively better. Since there is always a bit of differences within 5° in the CA's not only at no voltage but also at high voltage, two reverse paths, either 1–2 or 3–4, couldn't be matched each other and the hysteresis is inherently involved with it.

Here, however, we noted one noticeable feature that two receding CA data along the path 2 and 4 showed much more smooth variation and followed well to the theoretical prediction of Eq. (1) than those of advancing. By utilizing this property we were able to obtain the very high reversibility and reproducibility: applying the cyclic continuous voltage along two distinct cyclic paths either composed of 2–3–4–1 starting at the highest electric potential or 4–1–2–3 starting at the lowest electric potential, we were able to remove the hysteresis completely for a few cycles (not shown since the data were strongly overlapped).

To explain this directional voltage dependence, it is possible to assume a plausible model that there exists the correction between the drop motion and the type of friction forces related to the surface roughness on AF 1600 film. Under applied continuous voltage, the drop moves with the constant dynamic friction so that the constant net force acts on the drop. As a result the variation of CA is continuous even under low voltage as shown in path 2 and 4. On the other hand, under the discrete applied voltage, the discontinuous static friction acts on the drop, i.e., the resistive linear electromechanical force induced by the external electric field acts on the drop until the drop just starts to move with the maximum static force, causing the discontinuous CA in path 1 and 3. In some literatures these differences dependent on the process along voltage direction were pointed out due to ion adsorption to the interface.^{2,15} Therefore they suggested AC voltage for reduction of these directional differences instead of DC voltage.

During applying the voltage, the center of mass of a drop was slightly movable causing the unstable position of the drop. Note that the center was not related to the position of Pt-electrode. Stabilizing this mobility is one of hard technical problems in EWOD so that it should, if possible, be suppressed or minimized since the unstable mobility is not desirable in the most applications of EWOD.^{6,9} However, this mobility maybe be preferable in the actuation of drops with EWOD.¹²

To test the reproducibility of EWOD, the CA measurements had been repeated only one sample. After 100 cycles

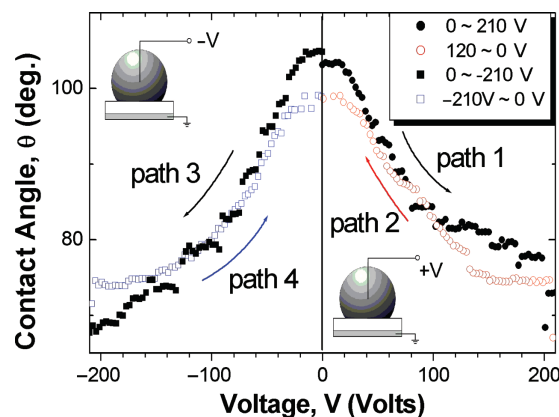


Fig. 6. The CA data after 100 cyclic EWOD measurements: hysteresis was much suppressed.

the experimental data along 4-different paths are presented in Figure 6. There was the reduction in the electrocontrollable CA range from 30 to 20°. One interesting feature is that not only reproducibility but also symmetry are preserved. Moreover the hysteresis in reversible processes disappeared remarkably but not completely. This result strongly supports the model of ion adsorption for hysteresis, because the surface roughness cannot be significantly changed during these cyclic measurements.

4. CONCLUSION

We studied experimentally the properties of EWOD on the hydrophobic surface of AF 1600 either with or without a high dielectric parylene-C film, with a specific applying voltage scheme. We were able to achieve the significant enhancement in the reversibility and the reproducibility of CA by driving the DC voltage continuously with starting from the highest absolute electric potential. Consequently it promises the precise control of the morphological deformations and the dynamic motions of micro-size liquid drops based on the EWOD technique.

Acknowledgments: This work was supported by the Nuclear Research R&D Program, the Mid-career Researcher Program (2011-0017539), the Nano/Bio Science and Technology Program (2005-01333), Sogang University Research Grant and the R&E Program of KSA, PET Converging Research Center Program, and a GIST-NCRC grant (R15-2008-006) funded by MEST, Korea.

References and Notes

1. G. Lippmann, *Ann. Chim. Phys.* 5, 494 (1875).
2. H. J. Verheijen and M. W. J. Prins, *Langmuir* 15, 6616 (1999).
3. C. Quilliet and B. Berge, *Curr. Opin. Colloid Interface Sci.* 6, 34 (2001).
4. F. Mugele and J.-C. Baret, *J. Phys.: Condens. Matter.* 17, R705 (2005).

5. J. Heikenfeld and M. Dhinda, *J. Adhes. Sci. Technol.* **22**, 319 (2008).
6. S. Berry, J. Kedzierskia, and B. Abedian, *J. Colloid Interface Sci.* **303**, 517 (2006).
7. B. Raj, M. Dhinda, N. R. Smith, R. Laughlin, and J. Heikenfeld, *Langmuir* **25**, 12387 (2009).
8. J.-T. Feng, F.-C. Wang, and Y.-P. Zhao, *Microfluidics* **3**, 022406 (2009).
9. B. Berge and J. Peseux, *Eur. Phys. J. E* **3**, 159 (2000).
10. E. Seyrat and R. Hayes, *J. Appl. Phys.* **90**, 1383 (2001).
11. S. Berry, J. Kedzierski, and B. Abedian, *Langmuir* **23**, 12429 (2007).
12. M. Paneru, C. Priest, R. Sedev, and J. Ralston, *J. Phys. Chem. C* **114**, 8383 (2010).
13. L. Meng, E. Liang, J. Gao, V. Teixeira, and M. P. dos Santos, *J. Nanosci. Nanotechnol.* **9**, 4151 (2009).
14. S. Hwang, T. Kim, J. Yoon, Y. Cha, Y. Kim, T. Seong, L. Kang, and S. Nahm, *J. Nanosci. Nanotechnol.* **11**, 884 (2011).
15. A. Quinn, R. Sedev, and J. Ralston, *J. Phys. Chem. B* **109**, 6268 (2005).

Received: 20 November 2010. Accepted: 11 March 2011.

Delivered by Ingenta to: Nanyang Technological University
IP: 37.9.47.89 On: Tue, 07 Jun 2016 17:31:10
Copyright: American Scientific Publishers